We are IntechOpen, the world's leading publisher of Open Access books
Built by scientists, for scientists

6,900
Open access books available

186,000
International authors and editors

200M
Downloads

154
Countries delivered to

Our authors are among the

TOP 1%
most cited scientists

12.2%
Contributors from top 500 universities

CLARIVATE ANALYTICS
BOOK CITATION INDEX
INDEXED

WEB OF SCIENCE™

Selection of our books indexed in the Book Citation Index
in Web of Science™ Core Collection (BKCI)

Interested in publishing with us?
Contact book.department@intechopen.com

Numbers displayed above are based on latest data collected.
For more information visit www.intechopen.com

Experimental Analyses and Numerical Models of CLT Shear Walls under Cyclic Loading

Valeria Awad, Linda Giresini, Mikio Koshihara,
Mario Lucio Puppio and Mauro Sassu

Additional information is available at the end of the chapter

Abstract

This paper reports the results of an experimental campaign performed at the University of Tokyo on cross-laminated timber (CLT) panels subjected to lateral loads. Analytical and numerical interpretations are provided as well, comparing the experimental analysis results with two methods: firstly, an analytical method to preliminarily evaluate the ultimate strength of the four panels, based on the geometrical dimensions of the openings and of the panel; secondly, a finite element model has been developed in order to provide some guidelines for calculating the stiffness and elastic behaviour of CLT panels subjected to lateral loads. The experimental tests showed that the CLT panels are as more brittle and stiffer as more the difference between the total panel area and the fenestrated area is high. The presence of large openings determined stress concentration at the corners where failure occurred for the attainment of the maximum tension strength in the inner layer. The proposed analytical formulation was shown to fairly closely predict the ultimate strength of panels with same geometry, characteristics and boundary condition, allowing preliminary information of this relevant parameter.

Keywords: cross-laminated timber, CLT, cyclic tests, shear walls, cut-out openings, FE model

1. Introduction

Cross-laminate timber, also identified as CLT or X-lam, is a relatively new technology widely used in Europe since the early 2000s. In the last few years, the use of CLT system in countries such as United States, Canada and New Zealand has improved bringing hundreds of impressive

buildings and showing that timber constructions, together with other natural materials [1], can be competitive, particularly for mid-rise and high-rise buildings. However, no specific design codes for CLT constructions were provided in Europe while Canada and United States have only recently published a CLT Handbook (US and Canadian version [2]) that provides key technical information related to manufacturing, design and performances of CLT, providing support for design and construction of CLT systems as alternative solutions in building codes. In Europe, Eurocode 5 governs the design of timber structures [3] and Eurocode 8 gives indications specifically related to seismic design [4]. In the literature, many contributions offer different interpretations of CLT panels subjected to lateral loads [5–8]. Nevertheless, in Japan, where timber buildings cover 50% of the constructions, a practical structural design of CLT buildings is not yet issued. To establish the law on the design method of CLT constructions suited with the Japanese regulations of seismic design, some research projects on CLT structures have been recently performed.

In the research field of CLT panels, an important contribute was given by the University of Ljubljana, Slovenia, where numerous quasi-static monotonic and cyclic tests were carried out on walls with lengths of 2.44 and 3.2 m and a height of 2.44 or 2.72 m [9]. Wall panels were subjected to gravity load induced by ballast as constant vertical load and a displacement-controlled hydraulic actuator as driver of the cyclic horizontal load. Moreover, for all the panels, three different cases of boundary conditions, from the cantilever type to the pure shear, were applied. These experiments have confirmed the importance of boundary conditions and the type of horizontal loading [10]. At a later stage, Dujic et al. [11–13] carried out other experimental and parametric studies to estimate the racking strength and stiffness of CLT wall panels with openings. Models were numerically tested by running non-linear static pushover analysis and results of calculations were compared with the test results. The experience conducted by Dujic et al. showed that cross-laminated panel with many openings has lower shear stiffness, but load-bearing capacity is not reduced as much, because failures are mostly concentrated in anchoring areas and in corners around openings with smashing and tearing of wood. Results were used to develop an exact mathematical model describing the relationship between the shear strength and stiffness of CLT wall panels without opening and panels with certain area of openings. An experimental study to quantify the seismic behaviour of X-Lam wall panels subjected to lateral loads was performed at the CNR-IVALSA Italian Institute [14]. The single-wall panels (2.95 × 2.95 m) included walls with openings and without openings and different connections layout and subjected to different levels of vertical loads. The results of these tests showed that the connections have a dominant role in the overall behaviour of the wall. As described in the Canadian edition of the CLT Handbook [2], in 2010, the FPInnovations Research Institute, in Vancouver, carried out 32 monotonic and cyclic tests [15]. The tests were conducted for 12 different configurations employing different wall-to-wall and wall-to-floor connections. As connectors, hold-down and brackets connectors were used, while as fastener, ring nails, spiral nails, self-threaded screws and timber rivets were utilized. Results of the experiments showed that CLT walls can have adequate seismic performance especially when hold-downs with nails on each end are used.

This paper deals with the interpretation of experimental tests carried out on full-size CLT panels with cut-out openings. The cyclic tests here described are performed on four three-layered 90-mm thick shear walls (30-30-30 mm) characterized by similar geometry, same boundary conditions and different cut-out openings. The experimental analyses results, performed up to timber and connection failures, were then compared with two methods. Firstly, an analytical method to preliminarily evaluate the ultimate strength of the four panels, based on the geometrical dimensions of the openings and of the panel, is proposed. Additionally, a finite element model has been developed in order to provide some guidelines for calculating the stiffness and elastic behaviour of CLT panels subjected to lateral loads.

2. Experimental tests on CLT three-layered panels

The experimental tests, carried out in the laboratories of the University of Tokyo, were addressed to specific aims. The first one was related to evaluating general performances of lateral-loading tests on four types of cross-laminated shear wall systems with openings. Additionally, effort was made to investigate the panels' response under cyclic loading, considering the influence of wood and connection features.

2.1. CLT panels and test set-up

The four test specimens of the full-scale CLT shear walls have openings (doors or windows, **Table 1**) and are three-layered 90-mm thick panels (30-30-30). The width of the one opening type is 4000 mm while the two opening panels are 6000 mm in width; their height is 2700 mm. These dimensions are displayed in **Figure 1**. From now on, the panels labelled in **Table 1** as 1S4-A, 1S4-B, 1S6-C and 1S6-D will be referred to as panels A, B, C and D, respectively. The panels are built in Sugi timber (Japanese cedar), which is characterized by a lower value of Young's modulus (4–6 GPa).

As example, panel C is displayed in **Figure 2a**. At the bottom of the wall, as shown in **Figure 2b**, two different types of connection between the panel and the steel foundation were used: the tensile connector and the shear connector. U-shaped steel elements with 12 screws each were adopted as tensile connections (**Figure 3a**) while U-shaped steel elements with 16 screws acted as shear connections (**Figure 3b**). The screws had a length of 65 mm and a diameter of 7 mm for all the joints.

Specimen	Opening type	Openings number	Length
1S4-A	Door	1	4 m
1S4-B	Window	1	4 m
1S6-C	Door	2	6 m
1S6-D	Window	2	6 m

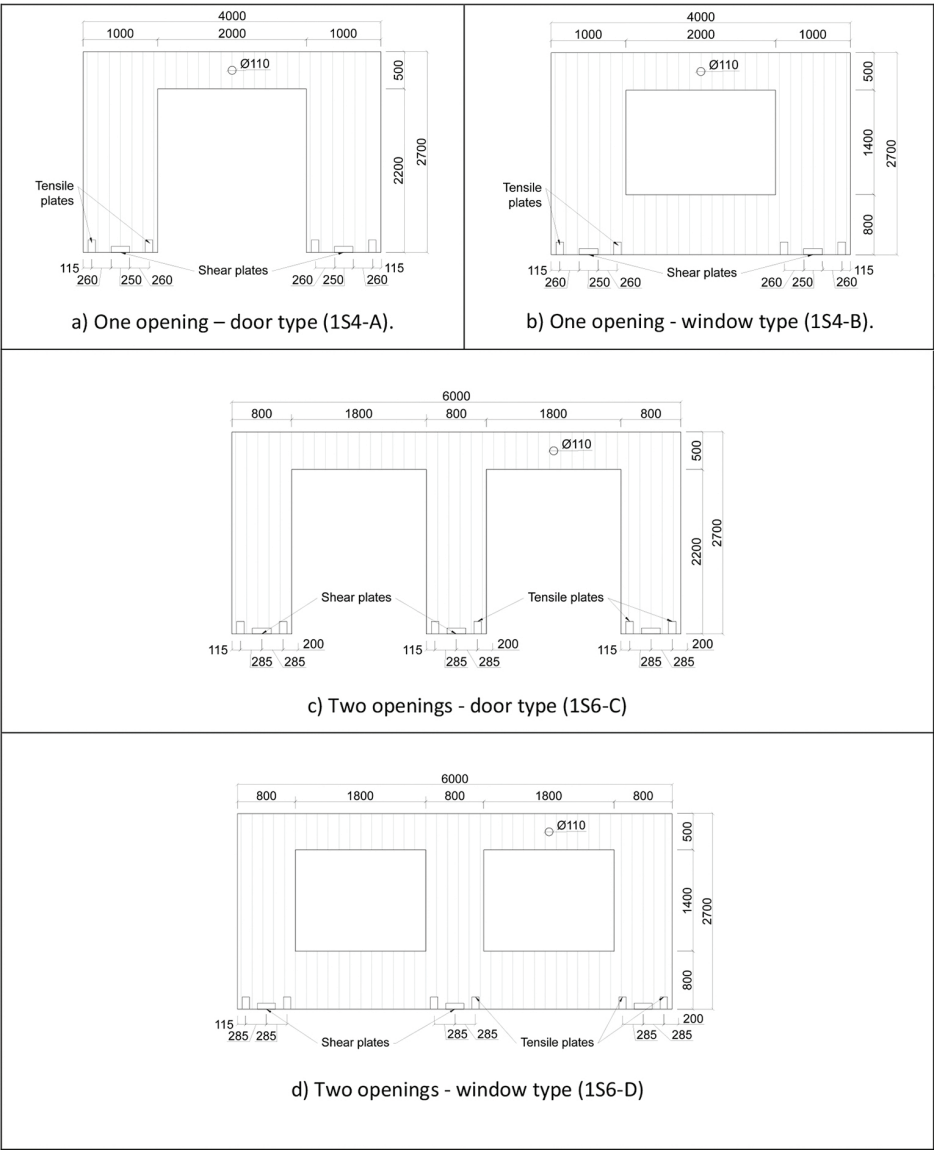**Table 1.** Labels and openings of the tested CLT panels.

Figure 1. Configuration and dimensions in mm of the tested CLT panels. (a) One opening—door type (1S4-A). (b) One opening—window type (1S4-B). (c) Two openings—door type (1S6-C). (d) Two openings—window type (1S6-D).

Figure 2. Two opening—door type (1S6-C): (a) overall view and (b) connection detail.
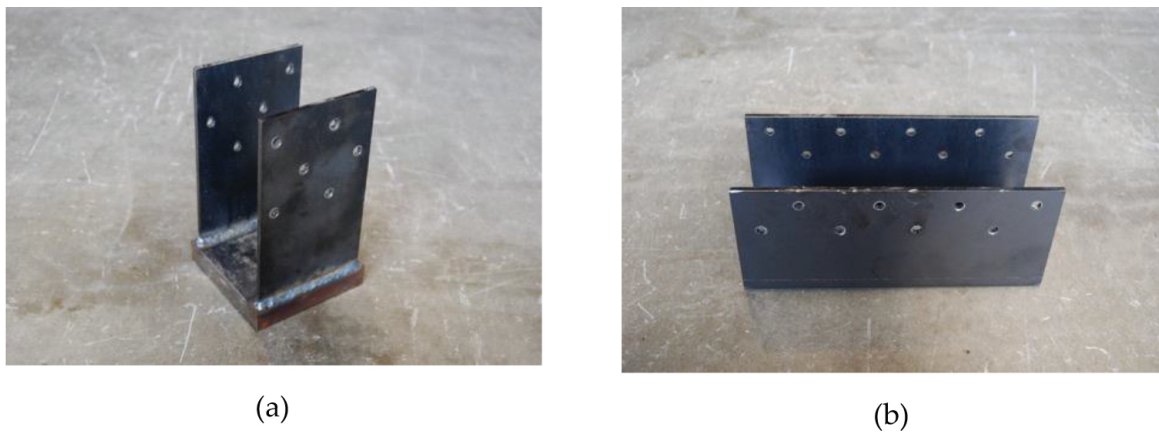
(a)

(b)

Figure 3. Connections: (a) tensile-type and (b) shear type.

The specimens were bolted down to a steel beam foundation with a double-tee Japanese profile (H300 × B300 × WT10 × FT15). The lateral load was applied to the pin joint of the CLT panels at a height of 2.450 m using a pair of oil jacks (**Figure 4**). 'C' steel-loading beams were bolted to the top of the CLT wall through a steel plate of 300 × 600 × 10 mm with screws with a diameter of 7 mm. In addition, lateral guides with rollers were used to ensure a steady and consistent unidirectional movement of the walls. Cyclic loading was applied with three cycles at each target deformation angle: 1/450, 1/300, 1/200, 1/150, 1/100, 1/75, 1/50 and 1/30 rad.
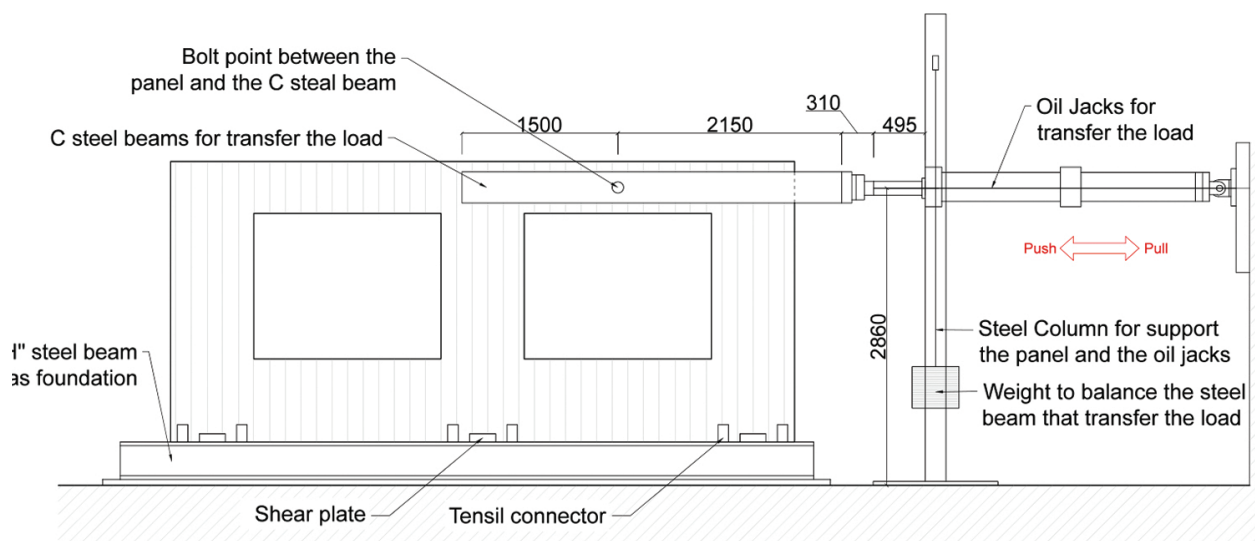

Figure 4. Experimental set-up (dimensions in mm).

Load was measured by the load cell set at the end of the oil jack, horizontal displacement of the panel at the height of loading points and near the bottom of the panel. Displacement transducers measured relative joint displacements (**Figure 5**). The axial strain of the bolt of each joint is measured using strain gauges.
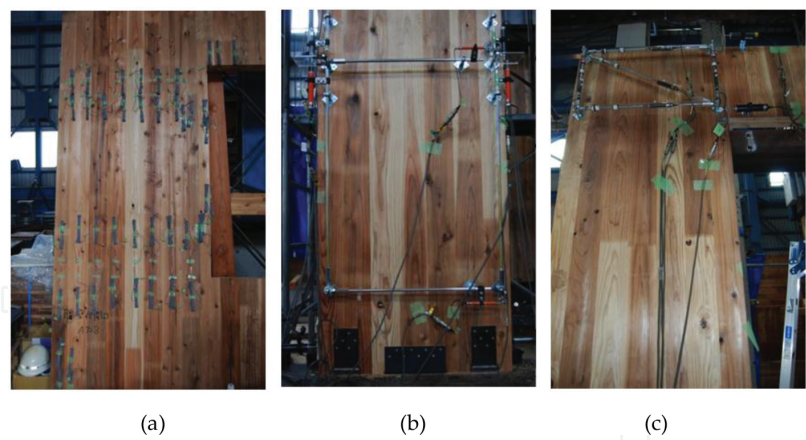
(a)   (b)   (c)

Figure 5. Measure instruments: (a) strain gauges applied on the lateral wall of the specimen 1S4-B4; (b) displacement transducer in the lateral walls and (c) displacement transducer at the joint point between lateral walls and beams.

The transducers were placed at the bottom and at the top of the panel (at a height of 2450 mm). The one at the top (**Figure 6**) allowed measuring the displacement of the entire panel, whereas the three at the bottom measured relative displacement between the wall base and the steel foundation. In the graphs P-δ that will be shown to present results, P is the shear load transferred from the two actuators while δ is the displacement defined as the difference of the translation at the top of the panel and the translation at the bottom of the panel, calculated as the average value given by the displacement recorded from Chapters 2 to 4 (**Figure 6**).
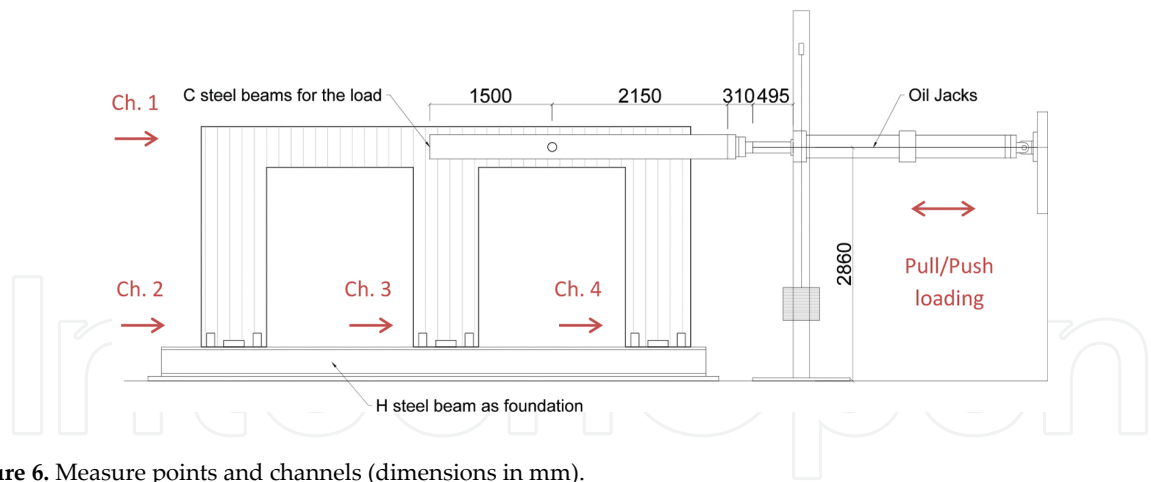

Figure 6. Measure points and channels (dimensions in mm).

2.2. Experimental tests results

2.2.1. Timber panels response

The cyclic tests results are reported and discussed in this paragraph. **Figure 7** summarizes the hysteresis curves obtained for each specimen specifying the cause of the failure and the crack position. **Table 2** reports the following elements:

– P_{max} is the maximum load derived from the load-deformation curve;

– δ_u is the ultimate deformation derived from the load-deformation curve;

– k_e is the value of the initial stiffness and is calculated as the slope of the line that connects the points of 0.2 P_{max} and 0.5 P_{max} on the hysteresis curve;

– P_y is the yield strength and is calculated as the value of the load at the point of intersection between the load-deformation curve and the 0.001-rad offset of the line corresponding to the initial value.
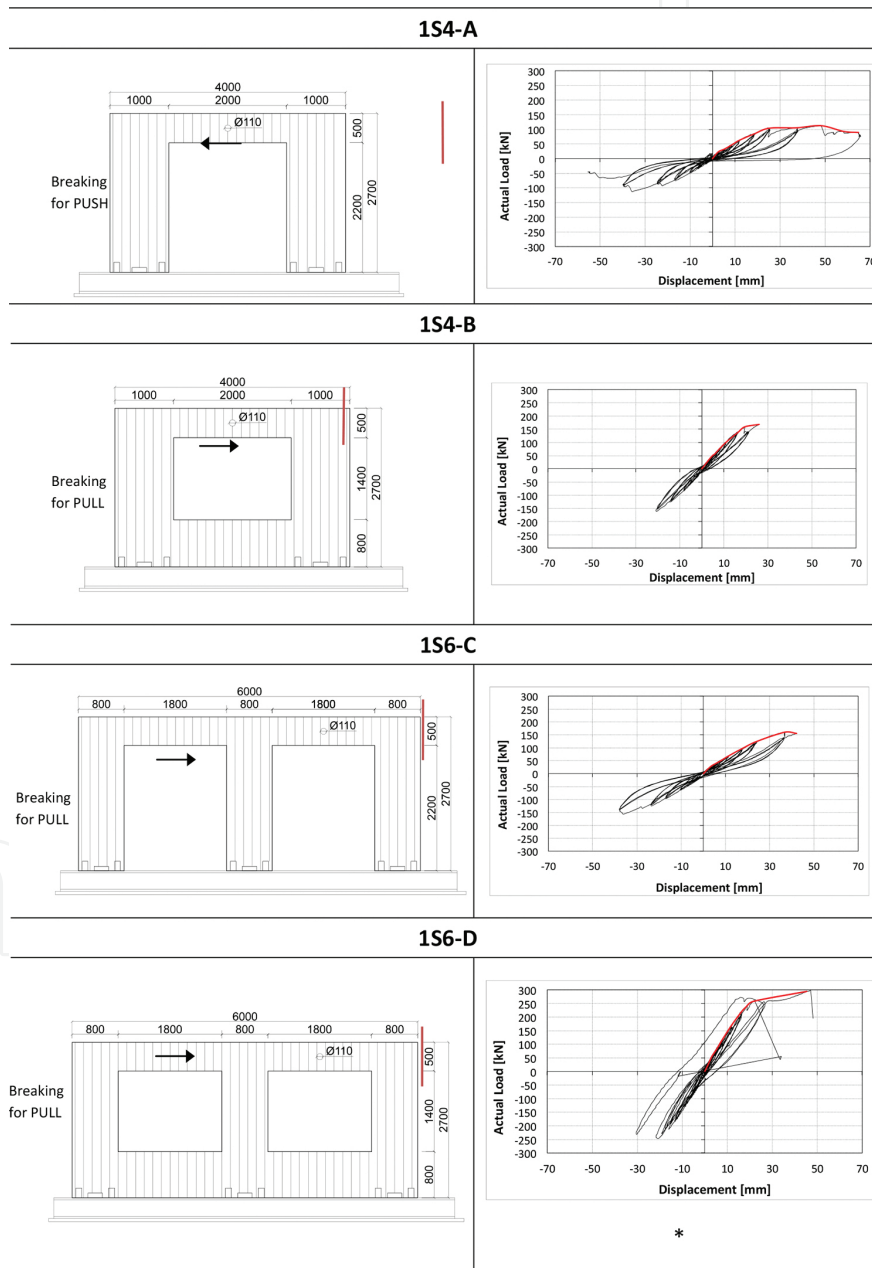

Figure 7. Test specimens and corresponding hysteresis curves (dimensions in mm). Backbone curve shown in red.

Specimen		P_{max} (kN)	δ_u (mm)	P_y (kN)	k_e (kN/mm)
One opening	1S4-A	112.43	65.89	103.40	4.21
	1S4-B	167.90	25.95	162.50	8.67
Two openings	1S6-C	160.60	42.15	149.61	4.99
	1S6-D	274.25	47.05	256.94	13.23

Table 2. Tabular results of the experimental tests (for the symbols meaning, see the body text).

For all the specimens, failure occurred at the upper corner of the opening and cracks always grew up from the corner of the opening to the top of the panel. The general behaviour was very brittle for all the panels with the exception of panel A for which a ductile behaviour can be recognized, entailing that the one-door-opening sample was also the one with the maximum dissipation of energy and the maximum deformation. The maximum strength was obtained for sample D but in this case the bending and sliding of the panel affected the data. Anyway, it can be observed that the maximum strength of the window type (panels B and D) is higher than that for the door type (panels A and C).

The initial stiffness k_e was calculated as the slope of the line that connects the points of 0.2 P_{max} and 0.5 P_{max} on the hysteresis curve. For calculating these values, the backbone curves of each hysteresis loop have been defined. The window types (panels B and D) showed a higher value of the initial stiffness k_e. Samples B and D are more resistant but allow lower deformations, whereas samples A and C have lower strength but higher deformations. Generally speaking, the backbone curve (**Figure 7**) represents the relationship between the maximum force and the corresponding deformation for each cycle of deformation angle to which the cyclic loading was performed. **Figure 8** shows the four backbone curves, allowing to compare the different behaviour of the wall-panel specimens.
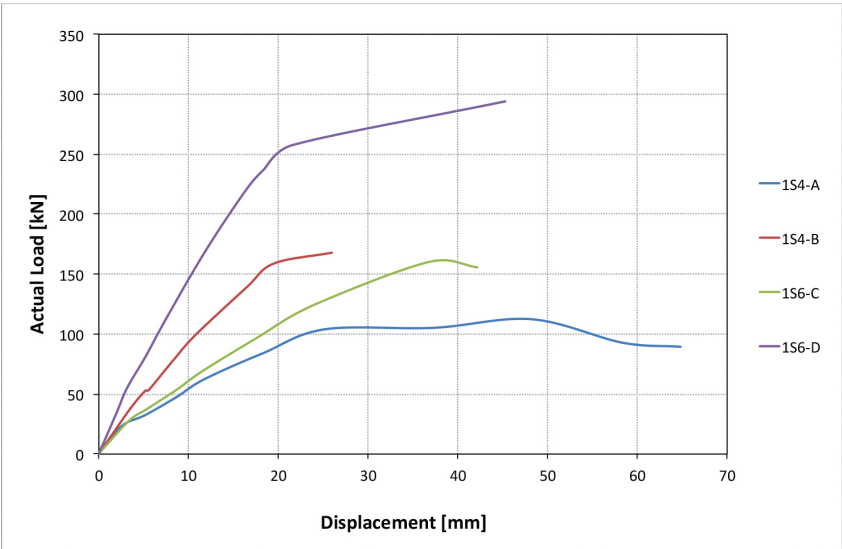

Figure 8. Comparison between the backbone curves of the four specimens.

The yielding strength was obtained as the point of intersection between the backbone curve and the line parallel to the initial strength and distant from this one of 2.45 mm in the graph. The value of 2.45 mm was calculated as 0.001 rad × 2450 mm, where 0.001 rad is given by the Japanese regulations and 2450 mm is the height of the top displacement transducer in the panel. The four wall panels have a prevalent brittle behaviour, except for specimen A that has a more ductile performance. Moreover, for all the four panels, it can be noted that the hysteretic loop has a typical pinched behaviour that is especially evident for panel A (**Figure 7**). In this case, in fact, the behaviour of the specimen, characterized by the presence of a wide open, was more affected by the behaviour of the connections than for other panels. As it will be discussed later, the screws used for panel A, after the test, were irreversibly damaged and their movement during the experiment caused the ovalisation of the holes. Thus, for panel A, during the model phase, the pinching effect, the degradation of stiffness and strength cannot be neglected.

2.2.2. Connections response

The configuration of the openings and the layout and design of joints strongly influenced the overall behaviour of a CLT structural system. For panels B, C and D, where the ratio between the openings area and the total area of the panel was lower than that for panel A, the overall response was ruled by the timber role. Moreover, for this panel the behaviour of the connectors largely affected the response of the specimen to lateral load, even if the failure is caused by the failure at the corner of the opening. It can be assessed that the connectors have basically all the same behaviour: they have a very stiff performance for the first cycles of the test, but, due to the wood crushing around the nails, their stiffness widely decreases during the experiment. The maximum strength is always around the same value, showing that although the connectors do not break, they all reach the yielding point. Moreover, their behaviour confirms that each connector has a negligible resistance to the tensile force that must be considered during the numerical model (Section 4) in order to correctly predict the rigid rotation and the stiffness of the specimens.

3. Analytical model

The load-bearing capacity and stiffness of fenestrated wood walls are mostly influenced by the size and layout of the openings. The reduction of strength observed during the experimental tests depends on the ratio of fenestrated area of the panel. Let us consider panels A and B, a wall without openings (index f). Let their ultimate strengths be, respectively, as P_A, P_B and P_f. One can suppose that the maximum strength of a panel with the same geometrical and boundary condition but with openings will be directly proportional to the value of P_f, namely:

$$P_A = P_f \times \alpha_A \tag{1}$$

$$P_B = P_f \times \alpha_B \tag{2}$$

where α_A and α_B are coefficients of <1. More in general this formula can be rewritten as:

$$P_n = P_f \times \alpha_n \tag{3}$$

For a generic panel with generic openings and boundary conditions, in order to find a bond between the strength and the geometrical values, the following considerations can be made:

- P_A and P_B will be directly proportional to the length $\Delta^{\underline{a}}$ of full-height wall segments and inversely proportional to the openings height;

From Eqs. (1) and (2), the ratio between P_A and P_B is equal to the ratio between α_A and α_B:

$$\frac{P_A}{P_B} = \frac{\alpha_A}{\alpha_B} \tag{4}$$

- The beams above and below the opening contribute in transferring load;
- All the panels have the same height and similar openings.

$$[P_A \cdot (h_A L_A - h_A b_A)] : b_A = [P_B \cdot (h_B L_B - h_B b_B)] : b_B \tag{5}$$

$$\frac{P_A}{P_B} = \frac{b_A}{b_B} \cdot \frac{h_B(L_B - b_B)}{h_A(L_A - b_A)} \tag{6}$$

Therefore, the following analytical formulation is proposed: where b and h are, respectively, the width and the height of the openings, while L is the width of the panel (**Figure 9**). P is the maximum shear strength attained by each panel during the experimental tests with the exception of panel D, whose value is not the one given by the experiment but the one corresponding to a deformation of 30 mm that, looking at the P-δ curve (**Figure 8**), and comparing its behaviour with the other three panels, seems more reliable.
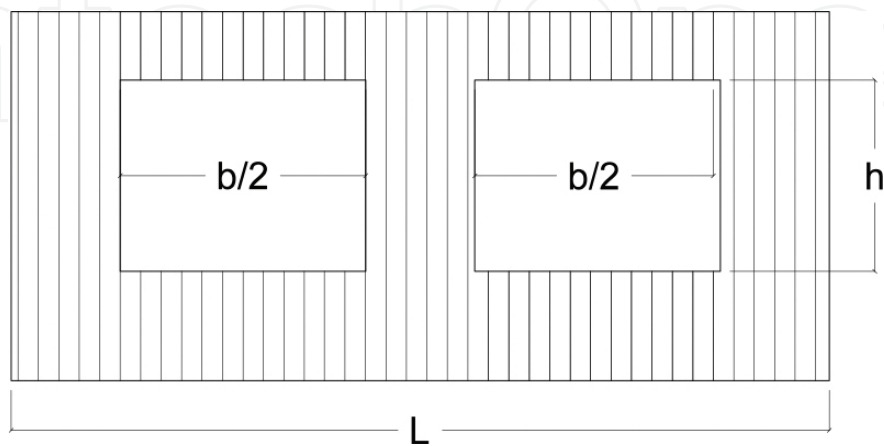

Figure 9. Symbols for the formulation of the ultimate strength in the analytical model.

The geometrical dimensions for the tested panels are reported in **Table 3**. **Table 4** shows the application of the proposed analytical expression for the four panels that have been tested in Tsukuba. The ratio between the ultimate strength of two panels determined during the experimental session is compared with the value obtained by comparing the geometrical conditions.

Specimen		P (kN)	L (m)	b (m)	h (m)
One opening	1S4-A	112.42	4	2	2.2
	1S4-B	167.90	4	2	1.4
Two openings	1S6-C	160.64	6	3.6	2.2
	1S6-D	272.05	6	3.6	1.4

Table 3. Mechanical and geometric data for each tested panel.

$$\frac{P_A}{P_B} = 0.669 = \frac{b_A}{b_B} \cdot \frac{h_B(L_B - b_B)}{h_A(L_A - b_A)} = 0.636 \, e \% Error = 5.2\% \tag{8}$$

$$\frac{P_A}{P_C} = 0.699 = 0.667 \quad \% Error = 4.8\% \tag{9}$$

$$\frac{P_A}{P_D} = 0.413 = 0.424 \quad \% Error = 2.6\% \tag{10}$$

$$\frac{P_B}{P_C} = 1.045 = 1.048 \quad \% Error = 0.3\% \tag{11}$$

$$\frac{P_B}{P_D} = 0.617 = 0.667 \quad \% Error = 7.5\% \tag{12}$$

$$\frac{P_C}{P_D} = 0.590 = 0.636 \, 0\% Error = 7.2\% \tag{13}$$

Table 4. Application of the proposed formulation and errors between the analytical values and the experimental value.

The error given by the analytical value never exceeds 8%, showing therefore that the mathematical formulation can predict fairly closely the ultimate strength of panels with the same geometry, characteristics and boundary conditions. However, it must be noted that this relationship gives acceptable results when panels are similar. If configuration of the openings or dimensions of the compared panels such as height and thickness change and, for example, the openings are not symmetrical, the proposed equation is too simple and it will not lead to reliable results.

Moreover, no tests on no-fenestrated panels have been conducted, so it was not possible to compare the results with a common value P_f. Thus, the analytical formulation can be used only

if the ultimate strength of one of two panels is already known and the panels have the same height. The mathematical model proposed in this paragraph is based on rough calculations and is therefore very approximate; however, it can be interpreted as a way to provide first information about the tendency of the reduction of racking strength of CLT shear walls with openings.

4. Finite element model

4.1. Description and mechanical parameters

The tested panels were modelled in SAP2000 by using a two-dimensional (2D) schematization with *"Shell-Layered/Nonlinear"* model [16]. The material properties adopted in the finite element model are listed in **Table 5**.

Modulus of elasticity—lower value (N/mm²)	E_{low}	4200
MOE—average value (N/mm²)	E_{av}	5200
Maximum bending strength (N/mm²)	σ_b	11,6
Modulus of elasticity—outer layers (N/mm²⁰)	$E_1 = E_3 = E_h$	173.33
Modulus of elasticity—inner layer (N/mm²)	$E_2 = E_v$	5200
Rolling shear modulus (N/mm²)	$G_{12} = G_{23}$	100
Longitudinal shear modulus (N/mm²)	G_{13}	400
Tensile strength—minimum value (N/mm²)	6.1.1. σ_t	12
Tensile strength—average value (N/mm²)	σ_t	16
Density (kg/m³)	ρ	439
Poisson's coefficients	ν	0.35

Table 5. Material properties adopted in the finite element model.

Under lateral loads, the connectors exhibit two different mechanisms of deformation. In the vertical direction, the anchors are subjected to tension, while in the horizontal one they experience shear deformation. These two deformation mechanisms are incorporated into the model by using individual springs for each of it, which act in unison. To find the stiffness and ultimate strength, tests on single-anchor elements should be conducted. In the present case, only the tensile connector (UT) has been previously subjected to monotonic load tests to correctly define its behaviour when subjected to tension.

The stiffness, strength and ductility of the steel connections are determined according to the Yasumura and Kawai procedure [17]. This procedure was initially proposed for the evaluation of wood-framed shear walls. The ultimate strength P_u is calculated so that the equivalence of the deformation energies is achieved by assuming an elasto-plastic load-displacement curve.

Figure 10 shows the definition of the bilinear curve that schematizes the behaviour of the tensile connectors. The contact—valid for tensile connectors—has been explicitly modelled using a set of compression-only springs identified at each point of the boundary mesh. For simulating the presence of the steel foundation, nodes with centre-to-centre distance of 10 cm have been generated at the base of the wall and all the degrees of freedom have been constrained. In the wall-to-floor contact, zero-length multilinear springs connect the nodes of the wall panel to the floor nodes. The compression-only springs are stiff in compression, and allow free movements away from it when subjected to tension. These springs are distributed along the contact between the wall and the floor. The friction between the steel beam foundation and the timber wall element is described by using spring elements with symmetrical and rigid-plastic behaviour placed along the whole length of the lower edge of the panel between the foundation nodes and the panel. The sliding resistance is described by the following equation:

$$F_f = k_f \bullet F_N \tag{7}$$

where F_N is the axial force at the current analysis step, k_f the static friction coefficient and F_f is the static friction force. The friction coefficient between the rough concrete and the CLT wooden surface was estimated as equal to 0.7 instead of the usual value of 0.4 used for two pieces of timber. In a proper schematization of the panel, the friction force should be calculated for each node taking into account the effective axial force that lies on each spring. Springs are stiff until the shear flow in the contact zone does not attain the estimated friction force. After this stage, friction springs have constant load-bearing capacity and resist sliding of panel in combination with non-linear springs that represent shear connectors.
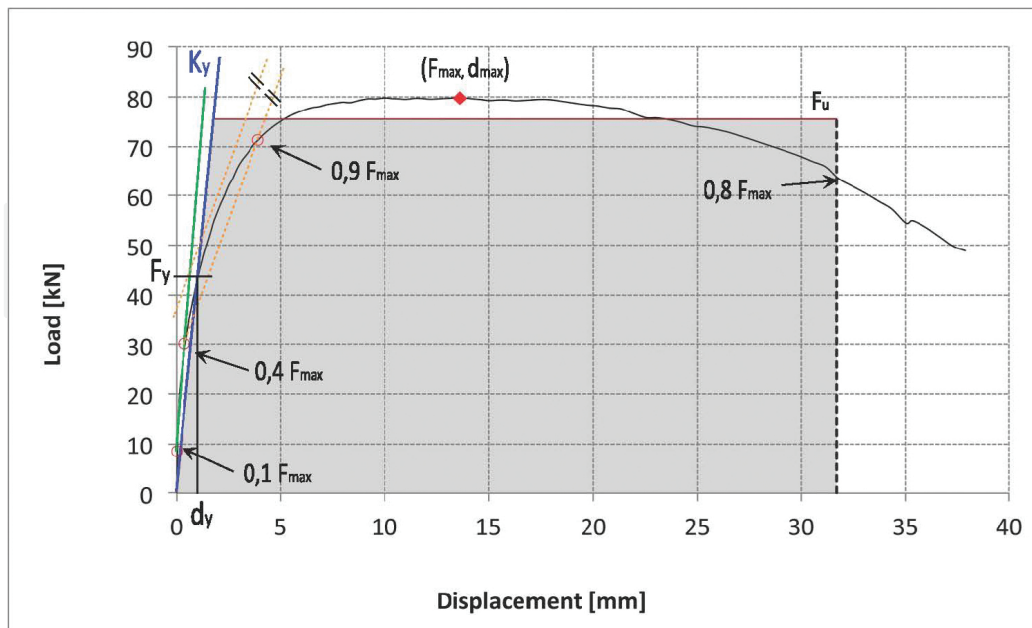

Figure 10. Definition of the bilinear curve (kN-mm) determined according to the *Yasumura and Kawai procedure* [17].

A pushover analysis was performed with a control of imposed displacement.

4.2. Results from finite element modelling

Confirming the experimental observation, the break occurs in the inner-cross layer due to the maximum tension attained in the corner of the opening of panel A (**Figure 11**). The maximum strength of 12 MPa is attained for a corresponding displacement of 17mm and 83-kN force.
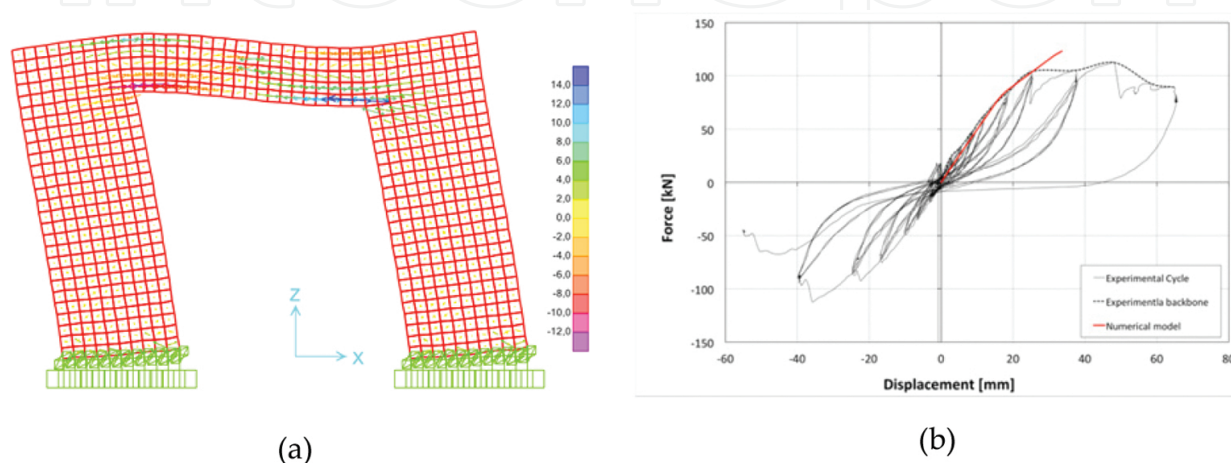

(a)   (b)

Figure 11. Panel A: (a) maximum and minimum tension stresses in MPa at the last analysis step; (b) numerical push-over curve compared to the experimental curve.

The force-deformation response obtained matches quite good to the experimental response for the elastic behaviour. When the panel starts to break and the behaviour became plastic, the CLT shear wall is subjected to large displacement for small increments of load.

For panel B, the upper left corner is the one where the break occurred, as seen in the experimental test (**Figure 12a**). **Figure 12b** shows the pushover curve obtained for the shear wall B. Panel B, contrary to panel A, has a very brittle behaviour. In this case, the yielding point is near the breaking point and an overall acceptable accuracy in terms of elastic stiffness was obtained. The presence of the sub-window increases the global stiffness of the panel and highlights again the relevant role of the boundary conditions (contact and friction). The overall behaviour of panel C, due to the absence of the sub-windows, depends strongly from the UT and US connectors.

In this case, the maximum tension is concentrated in both the external and internal corners as shown in **Figure 13a**. Due to the eccentric position of the load joint (located not in the geometrical centre of the panel but in the centre of the right window), the maximum tension that brought to failure occurred in the inner corner. **Figure 13b** shows the comparison between the backbone curve and the pushover curve with the observation that the numerical model results approximate the experimental ones quite well.
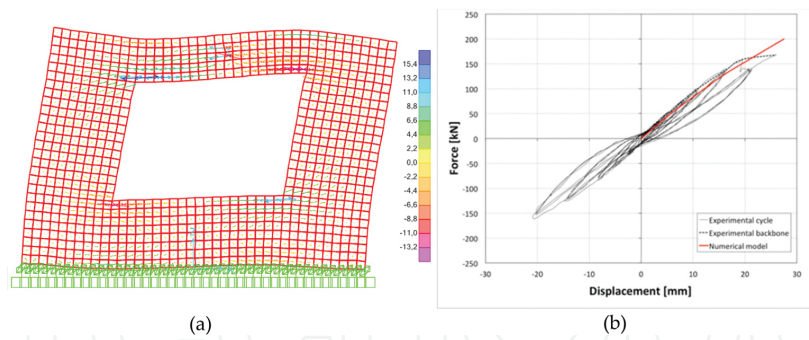
(a)   (b)

Figure 12. Panel B: (a) maximum and minimum tension stresses in MPa at the last analysis step; (b) numerical push-over curve compared to the experimental curve.
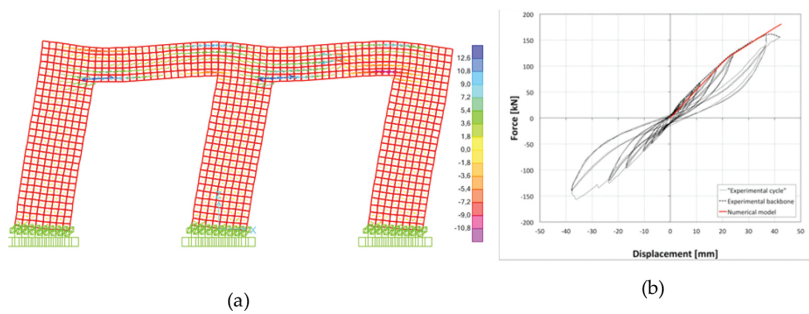

(a)   (b)

Figure 13. Panel C: (a) maximum and minimum tension stresses in MPa at the last analysis step; (b) numerical push-over curve compared to the experimental curve.

As shown in **Figure 14a**, the stress concentration occurs in the corners of the windows and the breaking point corresponds with the inner corner of the left window confirming the experimental results. Also in this case, the sub-window contributes to increase the overall stiffness behaviour. In contrast with the other cases, for panel D, the pushover curve does not approximate exactly the stiffness of the panel (**Figure 14b**). The main reason of this result can be founded both in the general errors that occurred in the experimental session and in the general approximation of the boundary conditions. Other numerical analyses could be aimed at evaluating the energy dissipated by panels during cycles as done for masonry buildings [18].
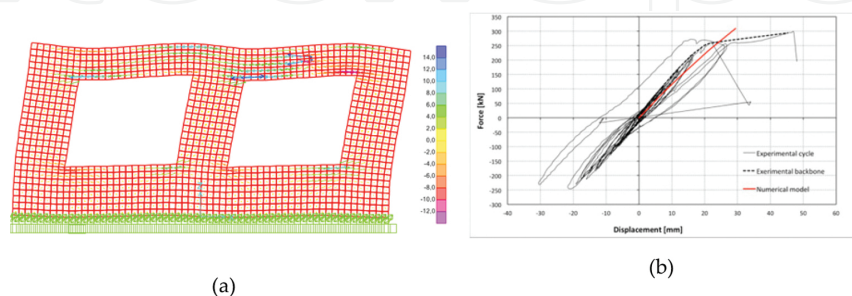

(a)   (b)

Figure 14. Panel D: (a) maximum and minimum tension stresses in MPa at the last analysis step; (b) numerical push-over curve compared to the experimental curve.

5. Discussion and comparison between results

The main results obtained from experimental tests on CLT panels with openings have been compared and interpreted through analytical and numerical models. Concerning the experimental tests, failure occurred at the upper corner of the opening for all the specimens. The general behaviour was brittle for all the panels with the exception of the panel with a one-door opening, the most ductile and also the one with maximum dissipation of energy and deformation. The maximum strength was obtained for the sample with two windows but in this case the bending and sliding of the panel affected the results. Anyway, the maximum strength of the window type (panels B and D) was observed to be higher than that for the door type (panels A and C). An analytical model was adopted to predict the ultimate strength of panels similar to the tested ones, knowing the ultimate strength of one of two panels and the panels have the same height. The error given by the analytical method never exceeded 8%, showing therefore that the mathematical formulation can predict fairly closely the ultimate strength of panels with the same geometry, characteristics and boundary conditions. Finite element models confirmed, in terms of failure type and crack position, the experimental results. Moreover, the pushover curve obtained from the finite element procedure generally matched the experimental one quite well. Further analyses could be addressed to evaluate the out-of-plane resistance of the timber panels, by means of rocking analysis with proper boundary conditions, applying analogous concepts adopted for masonry panels [19, 20].

6. Conclusions

An experimental campaign aimed at evaluating the ultimate behaviour of CLT panels with openings was here described and interpreted with both analytical and numerical models. The four-wall panels were shown to exhibit a prevalent brittle behaviour, except for the specimen with one-door opening, more ductile. This response was reproduced quite well in the multi-layered finite element model. The position of the cracks at the ultimate limit state was correctly obtained from the numerical procedure, highlighting that the failure occurs at the corner of the openings, in different position depending on their size and configurations. The analytical model was capable to correctly evaluate the values of ultimate limit strength of walls with cut-out openings, with errors lower than 8%.

Acknowledgements

Author details

Valeria Awad[1], Linda Giresini[1*], Mikio Koshihara[2], Mario Lucio Puppio[1] and Mauro Sassu[1]

*Address all correspondence to: linda.giresini@unipi.it

1 Department of Energy, Systems, Territory and Constructions Engineering (DESTEC), University of Pisa, Pisa, Italy

2 Department of Human and Social Systems, International Center for Urban Safety Engineering (ICUS), University of Tokyo, Tokyo, Japan

References

[1] Sassu, M., De Falco, A., Giresini, L., Puppio, M.L., Structural Solutions for Low-Cost Bamboo Frames: Experimental Tests and Constructive Assessments, Materials 2016, 2016, 9, 346; doi:10.3390/ma9050346.

[2] Handbook: cross-laminated timber (2011). Special Publication SP-528E, FPInnovations, edited by Gagnon S. and Pirvu C., QC, Canada.

[3] EN 1995-1-2 (Eurocode 5) (2004). Design of timber structures, Part 1-2: General—Structural fire design, CEN, Brussels, Belgium.

[4] Follesa, M., Christovasilis, I.P., Vassallo, D., Fragiacomo, M., and Ceccotti, A. Seismic design of multi-storey CLT buildings according to Eurocode 8. Ingegneria Sismica/International Journal of Earthquake Engineering, Special Issue on Timber Structures, Anno XXX-N.4 – Ottobre-Dicembre 2013.

[5] Studiengemeinschaft Holzleimbau e.V. Building with cross laminated timber. Load-bearing solid wood components for walls, ceilings and roofs. Published: 04/2010, 2nd edition: 01/2010, 2011.

[6] Fragiacomo, M, Dujic, B, Sustersic, I. Elastic and ductile design of multi-storey crosslam wooden buildings under seismic actions. Engineering Structures 33, 2011, 3043–3053.

[7] Rinaldin, G., Amadio, G., Fragiacomo, M., A component approach for the hysteretic behaviour of connections in cross-laminated wooden structures. Earthquake Engineering & Structural Dynamics 2013; 42: 2023–2042.

[8] Bogensperger, T., Moosbrugger, T., Silly, G., *Verification of CLT-plates under loads in plane*. Proceedings of the 11th World Conference on Timber Engineering, Riva del Garda, Italy, 2010.

[9] Dujic, B., Klobcar, S., Zarnic, R., Influence of openings on shear capacity of wooden walls. Research report, University of Ljubljana and CBD Contemporary Building Design Ltd., Slovenia, 2005.

[10] Dujic, B., Aicher, S., Zarnic, R., Investigation on in-plane loaded wooden elements – influence of loading on boundary conditions. Otto Graf Journal, Materialprüfungsanstalt Universität. Otto-Graf-Institut, Stuttgart, Vol. 16, 2005.

[11] Dujic, B., Hristovsky, Zarnic R. *Experimental investigation of massive wooden wall panel system subject to seismic excitation*. Proceeding of the First European Conference on Earthquake Engineering. Geneva, Switzerland, 2006.

[12] Dujic, B., Klobcar, S., Zarnic, R., *Influence of Openings on Shear Capacity of Wooden Walls*. In: Proceedings of the 40th CIB-W18 Meeting, paper 40-15-6, Bled, Slovenia, 2007.

[13] Dujic, B., Klobcar, S., Zarnic, R., *Shear capacity of cross-laminated wooden walls*. Proceedings of the 10th World Conference on Timber Engineering, Miyazaki, Japan, 2008.

[14] Ceccotti, A., New Technologies for Construction of Medium-Rise Buildings in Seismic Regions: The XLAM Case, Structural Engineering International: Journal of the International Association for Bridge and Structural Engineering (IABSE), n. 18, pp. 156–165, 2008.

[15] Popovski, M. Lateral resistance of cross-laminated wood panels. In: Proceedings of the 11th world conference on timber engineering. Vol. 4. Trees e Timber Institute, pp. 3394–3403, 2010.

[16] Sap2000 V.14, CSI, Computers and Structures Inc., CA, USA.

[17] Yasumura, M, Kawai, N. Evaluation of wood framed shear walls subjected to lateral load. Meeting 30 of the Working Commission W18-Timber Structures, CIB. Vancouver, Canada, 1997, paper CIB-W18/30-15-4, 1997.

[18] Giresini, L., Energy-based method for identifying vulnerable macro-elements in historic masonry churches, Bulletin of Earthquake Engineering. 2006, Volume 14, Issue 3, pp 919–942. doi: 10.1007/s10518-015-9854-7.

[19] Giresini, L., Fragiacomo, M., Lourenço, P.B., Comparison between rocking analysis and kinematic analysis for the dynamic out-of-plane behavior of masonry walls. Earthquake Engineering and Structural Dynamics. 2015, Volume 44, Issue 13, pp. 2359–2376, doi: 10.1002/eqe.2592.

[20] Giresini, L., Fragiacomo, M., Sassu, M. Rocking analysis of masonry walls interacting with roofs. Engineering Structures, 2016, Volume 116, pp. 107–120. doi: 10.1016/j.engstruct.2016.02.041.